JOURNAL OF PROPULSION AND POWER
Vol. 17, No. 3, May–June 2001

Aerothermal Model for Real-Time Digital Simulation of a Mixed-Flow Turbofan Engine

Vivek Sanghi,* B. K. Lakshmanan,† and R. Rajasekaran‡
Gas Turbine Research Establishment, Bangalore 560 093, India

This paper presents a way to simplify an explicitly time-integrated, aerothermodynamic transient model of a twin-spool, mixed-flow turbofan engine based on state variables and control volumes approach such that computational performance becomes suitable for real-time digital simulation. The key simplification lies in the modeling of main mixer, in which the mixing of core and bypass streams takes place. The number of state variables in an existing thermodynamic model has been reduced to six from nine by assuming that, instead of a uniform rate of static pressure rise, the static pressure is uniform across the main mixer. Computational time decreases primarily because the model is now less sensitive to pressure dynamics, thus allowing a larger integration time step. The accuracy of transient simulations is also less affected by artificial increases in actual physical size of control volumes, permitting further increase in integration time step. Numerical experiments show that simplified mixer modeling together with an increase in control volumes size by a factor of three resulted in an integration time step of 1.2 ms. It enables the model to run in real time on a state- of-the-art personal computer type of digital platform, without loosing the accuracy and numerical stability of the analysis. The formulation, validation, and real-time capabilities of the proposed methodology are discussed.

Nomenclature

A	=	area
G	=	differential equations vector
H	=	enthalpy
M	=	Mach number
m	=	mass
N	=	spool rotational speed
P	=	total pressure
p	=	static pressure
Q	=	flow function
R	=	gas constant
T	=	total temperature
TM	=	total momentum
T_s	=	static temperature
t	=	time
U	=	input vector
W	=	mass flow rate, $\dot{m}$
W_F	=	fuel flow rate
WRK	=	component work
X	=	state vector, time-scaling factor
$\dot{X}$	=	time derivative of X
γ	=	ratio of specific heats
Δ	=	change/error in a quantity
η_m	=	spool mechanical efficiency
σ	=	total pressure loss coefficient

Subscripts

ACC	=	engine accessories
avg	=	averaged value
BP	=	bypass duct
H, HP	=	high-pressure spool
HPC	=	high-pressure compressor
HPT	=	high-pressure turbine
L, LP	=	low-pressure spool
LPC	=	low-pressure compressor
LPT	=	low-pressure turbine
mx	=	main mixer
nz	=	nozzle
α	=	ambient conditions

Engine Station Designation

1	=	engine (fan/LP compressor) entry
2	=	fan (LP compressor) exit
3	=	HP compressor exit/combustor entry
4	=	HP turbine entry
5	=	HP turbine exit/LP turbine entry
6	=	LP turbine exit
7	=	nozzle entry
21	=	HP compressor entry
26	=	cold-stream main-mixer entry
42	=	HP turbine throat
52	=	LP turbine throat
61	=	hot-stream main-mixer entry
62	=	main-mixer exit upon mixing

Received 8 April 2000; revision received 24 July 2000; accepted for publication 5 January 2001.

*Scientist, Engine Simulation Division; vivek@drgtre.ren.nic.in. Senior Member AIAA.
†Head, Engine Simulation Division.
‡Scientist, Engine Simulation Division.

Introduction

AN ACCURATE understanding and prediction of engine steady-state and dynamic response is important for definition, development, and refinement of an engine control system and to have sufficient confidence in engine handling early during design. With the advent of computers, digital simulation has been used extensively for predicting engine response. It permits an in-depth understanding of an engine's dynamic and steady-state behavior and can be carried out at low cost, without endangering the engine.

An engine simulation program begins with the development of a nonlinear detailed thermodynamic mathematical model for predicting its dynamic and steady-state performance. Because of large-scale computations, it usually works in non real time. It is particularly useful in the early design phase and primarily aids in the development of controls logic and software.

Subsequently, the engine control system software is integrated with an engine thermodynamic model to develop a complete model of the process to be controlled and the control system itself. It serves as a cost-effective way of evaluating the dynamic behavior of the engine and control combined prior to any full-scale testing and enables the evaluation of the functional feasibility of control system software

by studying its interactions with the engine, i.e., closed-loop simulation so as to provide an increased understanding of the process dynamics.

Until this stage both the engine and control system are in software form and need to be translated into a hardware form. The dynamic response of control system hardware must be verified, prior to its integration, with actual engine hardware. The real-time simulation is an essential requirement to accomplish this task, in a "hardware-in-the-loop" simulation rig facility. Here, the engine is represented by a real-time software, to which the control system is integrated in the hardware form. Besides, real-time engine models are also useful for evaluation of integrated flight/propulsion controls, embedded models for flight systems, and for failure detection and accommodation.

The real-time simulation is a transient performance computer program whose engine outputs are generated at a rate commensurate with the response of the physical system it represents. Thus to realize the real-time simulation in practice, the cycle time (i.e., the computation time for one pass through the engine simulation model) must be shorter than the frame time (i.e., integration time-step size). Reference 1 gives a comprehensive description of various issues related to development and application of real-time engine models.

The real-time digital simulation can be accomplished using an aerothermodynamic model or else by piecewise linear transfer function or state-space models. The linear models, although simple and computationally fast, have limited scope because simulation is valid only for small movements about a single operating point. By scheduling the engine dynamic parameters against one or more engine variables, the model can be made valid for large disturbances, but a large amount of practical or theoretical work is necessary to obtain sufficient information prior to developing piecewise linear models. Also, any alternation in engine design requires redefining the entire model.

As indicated in Ref. 2, the aerothermodynamic model is preferred because it is more flexible, versatile, works over the entire engine operating range, and permits a greater insight into the engine dynamics. It is a better approximation of the actual thermodynamic processes in the engine, allows the behavior of any engine parameter to be determined during a transient, and effects such as bleed, blowoff, variable geometry, and thermal capacity can easily be incorporated. The design changes are also easily accommodated by simply changing the corresponding database.

The existing in-house developed detailed nonlinear thermodynamic simulation[3] does not have real-time capability because the computation time taken by it is a major drawback while implementing it even on a state-of-the-art digital computer. It is caused by the use of a simple explicit integration technique (i.e., Euler) to update the engine transient state. Small frame time of 0.1 ms is required to produce a stable system. This is especially true of the "stiff" systems like jet engines, which have widely varying time constants (0.10 ms to 1.0 s) for temperature, pressure, and rotor dynamics, respectively. The real-time simulation problem then becomes one of limiting the number of calculations by model simplification and/or increasing the frame time while preserving the dynamic accuracy and stability of simulation.

This paper first describes the existing nonlinear detailed thermodynamic model. Subsequently, the basis for reducing the number of state variables to six, associated increase in frame time, validation in steady state as well as in open- and closed-loop simulation setup, and its real-time capabilities are discussed.

Existing Detailed Nonlinear Thermodynamic Engine Model

The description contained in Ref. 4 has been used as the basis for developing the existing detailed nonlinear thermodynamic simulation model for a twin-spool mixed-flow turbofan engine with reheat. It is approached from the viewpoint of engineering thermodynamics, uses compressor and turbine characteristics, and is founded on the techniques of component matching. The effects of variable geometry are introduced into the model as corrections to the fixed geometry performance maps.

The thermodynamic behavior of every component is represented by a set of theoretical or empirical equations. The relationship between the components is fixed by the engine physical layout and by the thermodynamic behavior of each component. The inputs to the model are flight conditions and control parameters, i.e., fuel flow in the main and reheat combustion chambers, compressor variable geometry setting, and A_{nz}. A set of engine parameters called state variables defines the operating point of each component for prescribed inputs. The state vector for a twin-spool, mixed-flow turbofan includes P_2, P_3, P_5, P_6, p_{61}, P_{62}, T_{62}, N_L, and N_H. A typical model for a mixed-flow twin-spool turbofan engine is shown in Fig. 1.

Dynamic or Transient Analysis

At the prescribed flight condition the components' operation is found, using the control inputs and initial state vector. As a general

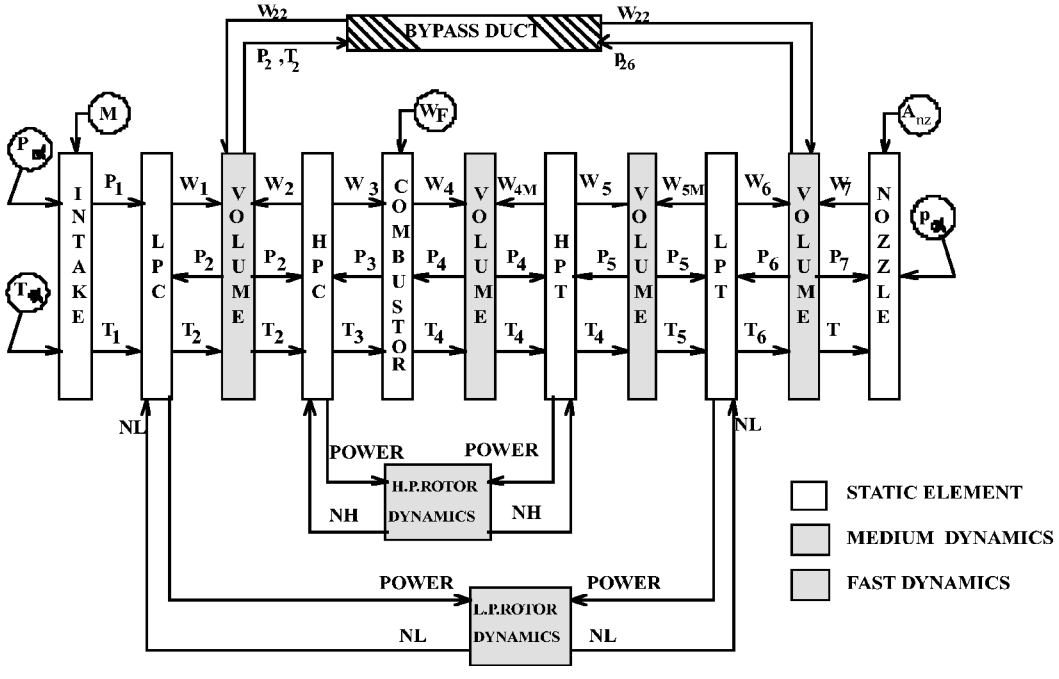

Fig. 1 Flow logic for a twin-spool, mixed-flow turbofan.

case, there will be a work imbalance (or a net torque on compressor-turbine assembly) and a flow mismatch (or mass accumulation) at various engine stations. The torque difference between the compressor and turbine on the same spool is used to generate the time derivative of rotational speed. The flow imbalance is treated using the intercomponent volumes method. Here, the individual components are interconnected by control volumes. The mass flow accumulation in control volumes is used to calculate the rate of pressures change with time ($\mathrm{d}P/\mathrm{d}t$) at various engine stations, where Vol is control volume and ΔW is the mass flow error in control volume.

$$P^* \equiv \frac{\mathrm{d}P}{\mathrm{d}t} = \frac{\gamma RT}{\mathrm{Vol}} \cdot \Delta W$$

The preceding equation is derived as follows:

$$p = \frac{mRT_s}{\mathrm{Vol}} \Rightarrow \dot{p} = \frac{R}{\mathrm{Vol}}(\dot{m}T_s + m\dot{T}_s)$$

The term $m\dot{T}_s$ is usually less than 20% of $\dot{m}T_s$ and hence is ignored.[4] The small Mach-number assumption makes it possible to replace static quantities (p and T_s) by total quantities (P and T). The resulting error in tracking the pressure dynamics caused by these assumptions will not significantly affect the model predictions. It is because the basic purpose of adopting the control volumes approach is to avoid iterations to obtain flow match, and the overall transient behavior is determined by the rotor dynamics as a result of its long time constant. The dynamics of pressure changes, which has a shorter time constant, is completed much earlier to the rotor dynamics. Thus an error in pressure dynamics shall only alter the compressor trajectory for a small duration, immediately following a change in control inputs.

The next engine state is computed by integrating time derivatives of state variables using the simple open Euler scheme:

$$X(t + DT) = X(t) + DT^*G(X, U, t), \qquad DT = 0.1 \text{ ms}$$

Choice of Control Volumes

The pressure dynamics, being faster than rotor dynamics, restricts the size of usable frame time in the solution of differential equations while updating the engine transient state. Small steps in time are necessary to track the engine dynamics accurately. One possible way to increase the frame time is to artificially dampen the pressure dynamics by choosing a relatively large control volume size. It permits a larger frame time (generally in the same proportion as increase in control volumes size) and hence a reduction in overall computing time. This procedure is termed as the time scaling of control volumes.

However, in the mixed-flow turbofan considered in this paper, increasing the control volumes size to increase the frame time introduces an error in the transient analysis. It is because the flow split between the bypass duct and the gas generator is sensitive to the changes in P_2 and p_{61} so that the pressure dynamics have a considerable influence on engine response.

The volume in the bypass duct and that between the low-pressure (LP) and high-pressure (HP) compressors is used to determine the derivative of P_2 and hence the P_2 update at the next time interval using the prescribed frame time. Because P_2 determines the pressure level in the bypass duct, it is one of the important parameters controlling the flow split between the bypass duct and the gas generator. The derivative computation of P_2 shall therefore be more accurate if actual physical volume is chosen.

The p_{26} is another parameter that controls the flow split at fan exit. Because $p_{26} = p_{61}$, p_{61} is a critical parameter. It has been used as a state variable, and its derivative is computed as given next. The ΔW_{62} is the mass flow accumulation in the control volume between main mixer and exhaust nozzle ($W_{61} + W_{26} - W_7$), and m_{mx} is the mass of the gas in the main mixer. Because of the critical nature of p_{61}, the term $m\dot{T}_s$ has been retained to improve the accuracy of $\dot{p}_{61}$ computation.

$$\dot{p}_{61} = \dot{p}_{62} = (R/\mathrm{Vol}_{\mathrm{mx}})\left(m_{\mathrm{mx}} * \dot{T}_{s,\mathrm{avg}} + \Delta W_{62} * T_{s,\mathrm{avg}}\right)$$

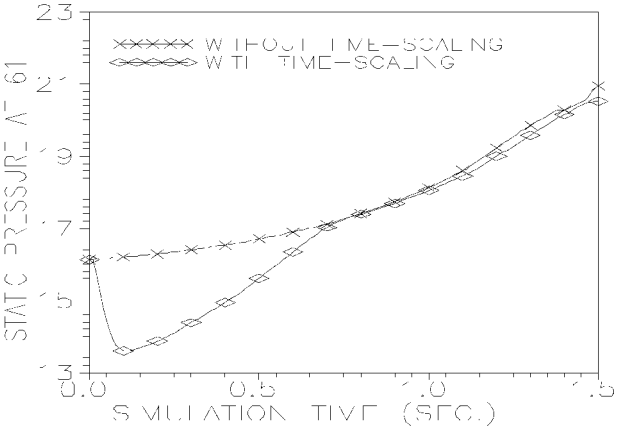

Fig. 2 Error in p_{61} with time scaling of control volumes.

In the preceding equation m_{mx} is computed as $p_{\mathrm{avg}} \cdot \mathrm{Vol}_{\mathrm{mx}}/R \cdot T_{s,\mathrm{avg}}$, and p_{avg} and $T_{s,\mathrm{avg}}$ are defined as $(p_{61} + p_{62})/2$ and $(T_{s,61} + T_{s,62})/2$, respectively. Because averaged p and T_S are assumed in the entire main mixer, the time derivative of static pressure at the entry station will take the same value as at the exit station. It is therefore reasonable to assume $\dot{p}_{61} = \dot{p}_{62}$, i.e., a uniform rate of static pressure rise across the main mixer.

Because $\Delta W^*_{62} T_{s,\mathrm{avg}}$, i.e., the second term inside the bracket is independent of control volume size, time scaling of control volumes will lead to erroneous computation of p_{61} derivative. As the control volume size is increased and a higher frame time is used, the derivative of p_{61} and hence its absolute value falls lower with respect to the baseline, which uses a frame time of 0.10 ms together with actual control volumes. It causes large errors in the transient path from the baseline. Because of these reasons, actual control volumes should be used in the digital simulation of transient performance with p_{61} as one of the state variables.

To illustrate this point, an open-loop transient was performed in which a ramp of 4.0 s was given to change the control variables (W_F and A_{nz}), causing the engine to accelerate from idling to max speed at sea-level static (SLS) in international standard atmosphere (ISA). It was possible to achieve a frame time of 0.5 ms with time scaling of control volumes by three times.

The difference in p_{61} update with and without time scaling of control volumes is indicated in Fig. 2. Only the first 1.5 s of the transient are shown because it is the initial phase during which the difference in p_{61} update is more noticeable. With an increase in frame time to 0.50 ms upon time scaling of control volumes by three times, the p_{61} update for the first 0.50 s of the transients is much lower compared to the baseline case (i.e., frame time of 0.10 ms with actual control volumes). Subsequently, the difference in p_{61} update reduces, but still the resulting p_{61} with time scaling of control volumes is on the lower side. This error in the p_{61} update also gets propagated in the update of remaining engine state variables, as a result of which an intermediate portion of engine rotor speed response deviates up to $\pm 3\%$ with respect to the baseline.

The computation time with three times the time scaling of control volumes (which permits an increased frame time of 0.50 ms) is $\approx$25 s for 20-s transients on a Pentium III machine. Therefore, even if an error up to $\pm 3\%$ is accepted, simulation is not in real time. Any further time scaling of control volumes to increase the frame time will only increase the error in transient path with respect to the baseline and may also introduce numerical instability.

Steady-State Analysis

For determining steady-state operation of a mixed-flow turbofan at the prescribed flight condition and control inputs, a total of nine errors contained in Table 1 are generated. The initial guess of state variables is continuously updated using the Multidimensional Newton–Raphson (MDNR) scheme until the summation of all of the errors comes within a prescribed tolerance band. The prefix U represents the upstream condition.

Table 1 Errors description for engine balancing using MDNR scheme

S.No.	Description[a]
1	$(UW_{21} - W_{21})/W_{21}$[b]
2	$(UW_{42} - W_{42})/W_{42}$[b]
3	$(UW_{52} - W_{52})/W_{52}$[b]
4	$(W_{26}^{c} + W_{61} - W_{62})/W_{62}$[d]
5	$(\eta_{m,\mathrm{LP}} * WRK_{\mathrm{LPT}} - WRK_{\mathrm{LPC}})/WRK_{\mathrm{LPC}}$
6	$[\eta_{m\text{-HP}} * WRK_{\mathrm{HPT}} - (WRK_{\mathrm{HPC}} + WRK_{\mathrm{ACC}})]/(WRK_{\mathrm{HPC}} + WRK_{\mathrm{ACC}})$
7	$(W_{26} * H_{26} + W_{61} * H_{61} - W_{62} * H_{62})/(W_{62} * H_{62})$
8	$(TM_{26} + TM_{61} - TM_{62})/TM_{62}$
9	$(UW_{61} - W_{61})/W_{61}$[e]

[a] $\sum_{i=1}^{9} \mathrm{error}_i \leq 0.0001$.
[b] W_1, W_{21}, W_{42}, and W_{52} are computed from maps, using corrected speed and pressure ratio.
[c] W_{26} is computed from $p_{26} = p_{61}$(state variable), $T_{26}(=T_2)$, P_{26} (P_2:state variable* σ_{BP}), and A_{26}.
[d] W_{62} is computed using the downstream A_{nz} and nozzle pressure ratio.
[e] W_{61} is computed from upstream P_{61}, T_{61}, p_{61} (state variable), and A_{61}.

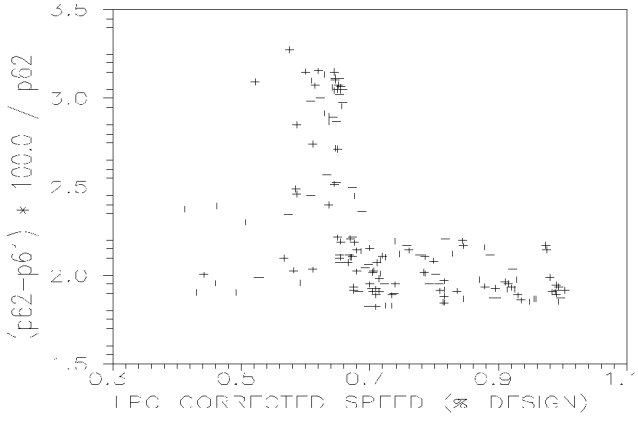

Fig. 3 Deviations between p_{62} and p_{61} during steady state.

Modified Detailed Model

The existing detailed engine simulation, as described earlier, is based on the assumption that the rate of static pressure rise is uniform ($\dot{p}_{61} = \dot{p}_{62}$) across the main mixer in which bypass air mixes with the core flow. This assumption introduces the use of p_{61}, T_{62}, and P_{62} as state variables to compute the derivative of state variable p_{61} during the transient analysis.

If the steady-state solution at a large number of flight points (with various throttle settings at each flight point, varying from idling to max speed as well as the reheat mode) is observed for absolute values of p_{61} and p_{62}, there is not a considerable difference between their magnitude. As can be seen from Fig. 3 that p_{62} in general is 2 to 3% more than p_{61}.

Similarly, deviations between p_{62} and p_{61} were observed to be within 1.50–2.50% for a number of open-loop transient paths with frame time of 0.10 ms for a step or ramp change in control variables (fuel flow and nozzle area) from the initial to final steady-state point. As a typical example, Fig. 4 contains the deviation between p_{62} and p_{61} for an open-loop transient at ISA, SLS condition in which a ramp of 4.0 s was given to change the control variables, causing the engine to accelerate from idling to max speed.

So it is appropriate to assume that static pressure itself is uniform across the mixer ($p_{62} = p_{61}$), instead of a uniform rate of static pressure rise. With this simplification use of p_{61}, T_{62}, and P_{62} as state variables is no more needed, and the total number of state variables are reduced to six. The modified engine model henceforth will be termed as the six state variables (6 s.v.) model, whereas the original engine model is the baseline nine state variables (9 s.v.) model.

Dynamic or Transient Analysis

The control volumes approach as described earlier is also used with the modified 6 s.v. model. The only difference is that parameters

Table 2 Modified errors description for engine balancing using MDNR scheme

S.No.	Description[a]
1	$(UW_{21} - W_{21})/W_{21}$
2	$(UW_{42} - W_{42})/W_{42}$
3	$(UW_{52} - W_{52})/W_{52}$
4	UW_7/W_7
5	$(\eta_{m,\mathrm{LP}} * WRK_{\mathrm{LPT}} - WRK_{\mathrm{LPC}})/WRK_{\mathrm{LPC}}$
6	$[\eta_{m\text{-HP}} * WRK_{\mathrm{HPT}} - (WRK_{\mathrm{HPC}} + WRK_{\mathrm{ACC}})]/(WRK_{\mathrm{HPC}} + WRK_{\mathrm{ACC}})$

[a] $\sum_{i=1}^{6} \mathrm{error}_i \leq 0.0001$.

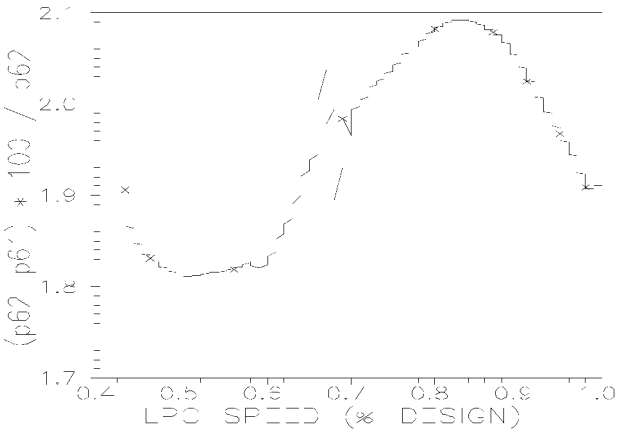

Fig. 4 Deviations between p_{62} and p_{61} during open-loop transients.

p_{61}, T_{62}, and P_{62} are now computed directly, instead of being updated subsequent to derivative calculation.

Knowing the engine state and mixer geometry at station 61, p_{61} is computed. The bypass duct mass flow is computed by imposing static pressure equality at main-mixer inlet ($p_{26} = p_{61}$). The resulting mass flow accumulation in the bypass duct is then used to generate the derivative of state variable P_2. The main-mixer exit mass flow rate, total temperature, and total pressure (i.e., W_{62}, T_{62}, and P_{62}) are computed by imposing mass flow, enthalpy, and momentum balance between the core and bypass flow. The W_{62} (together with bleed-air mixing, if any) is then compared with the nozzle entry mass flow (computed using the prescribed nozzle area as a control input). The resulting mass flow accumulation (ΔW_{62}) is used to generate the derivative of P_6. The derivative computation of remaining state variables (P_3, P_5, N_L, and N_H) remains the same.

Steady-State Analysis

Similar to the 9 s.v. model, the initial guess of state variables is continuously updated using the MDNR scheme until the summation of all of the errors comes within a prescribed tolerance band. Because the number of state variables is reduced to six, only six errors need to be generated. The modified error matrix for identifying engine steady state at a given flight point and for the prescribed control inputs is indicated in Table 2.

Frame-Time Estimates

The primary objective with which the 6 s.v. formulation is attempted is to explore the possibility of developing a detailed nonlinear thermodynamic simulation, which runs in real time on a state-of-the-art PC. Because any further model simplification will not be a true representation of engine thermodynamic process, attempts were made to investigate the possible increase in frame time to achieve real-time simulation. For this purpose an open-loop transient was performed at ISA, SLS, for a 4.0-s ramp change in control variables that corresponds to engine excursion from idling to max speed in dry mode.

The maximum achievable frame time with time scaling of control volumes such that there is not any considerable distortion in engine transient path with respect to the baseline 9 s.v. case, which uses a

Table 3 Computation time vs frame time

Time-scaling factor	DT, s	Computation time, s	Error from baseline,%
1	0.0004	33.09	±1.25
2	0.0008	16.69	±1.50
3	0.0012	11.10	±1.75
4	0.0016	08.35	±4.00
5	0.0020	06.70	±5.00

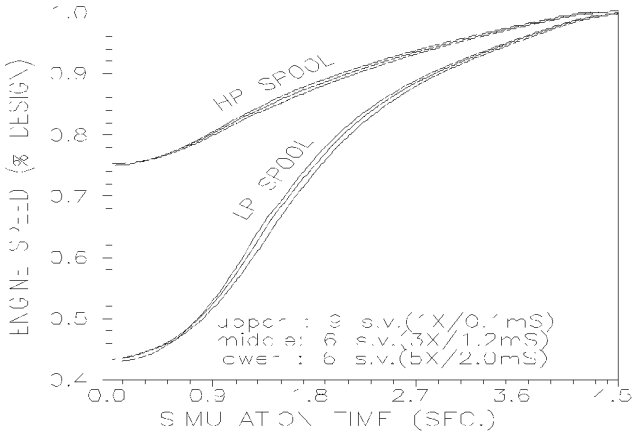

Fig. 5 Sensitivity of frame time.

frame time of 0.10 ms with actual control volumes, is contained in Table 3. The reference for overall computation time is a Pentium III machine for a 20-s transient. Error indicates the maximum error in LP spool speed with respect to the baseline, and a similar error shall exist in other engine state parameters as well. This error was observed only in an intermediate portion of the transients during the first few seconds. The final steady-state point upon completion of the transients was the same for all of the frame times shown in Table 3.

The proposed 6 s.v. model permits a frame time of 0.40 ms (as against 0.10 ms in the baseline 9 s.v. model), with a further increase being possible by time scaling of control volumes. A frame time of 1.2 ms upon time scaling of control volumes by three times was found to be quite accurate as well as numerically stable for performing open-loop transient analysis at other flight points as well. It also enables the digital simulation to be in real time on an overall basis. As a limiting case, the frame time could be increased to 2 ms with five times the time scaling of control volumes, provided errors up to ±5% with respect to the baseline 9 s.v. model can be accepted.

The comparison of the transient path at frame times of 1.2 and 2.0 ms with three (3X) and five (5X) times the time scaling of control volumes respectively with baseline 9 s.v. model is shown in Fig. 5, to illustrate the trends of Table 3. Only that portion is shown where difference is more prominent.

Unlike the 9 s.v. model, p_{61}, instead of being a state variable, is now actually computed at each time interval based on engine state at station 61 and the mixer geometry. Also, the p_{61} computation does not include any control volume term and is independent of control volumes size. As a typical example, with time scaling of control volumes by three times and for a frame time of 1.2 ms, p_{61} is within ±2% in comparison to that obtained from the baseline 9 s.v. model at all of the points of the earlier-mentioned ISA, SLS transient. The 6 s.v. model is therefore less sensitive to pressure dynamics and time scaling of control volumes, thereby allowing the use of higher frame times.

Limits on Control Volumes Time Scaling

The results of Table 3 indicate that there is a limit to which the control volumes can be time scaled. It is not possible to indefinitely increase the control volumes size to increase the frame time, as it reduces the accuracy and numerical stability of transient analysis.

Consider two transient analysis cases to illustrate this point. The first case uses a frame time of 0.40 ms, without any time scaling of control volumes. In the second case a frame time of $x * DT (DT = 0.40$ ms) is used, upon x times the time scaling of control volumes. The first case will need an update of x times in comparison to the second one (which needs to be updated only once) to reach the same time interval after the transient is initiated.

Irrespective of the control volumes size, the initial steady-state point will be the same for prescribed control inputs at a given flight point. At $t = 0$ the derivatives of all of the pressure terms in the state vector for the second case are $1/x$ times of their respective values in the first case. There will be no change in the values of these pressure derivatives until the engine reaches a time interval of $x * DT$ s from start in the second case. But the pressure derivatives will change at every DT in the first case. Thus, time updates of all of the pressure terms at the end of $x * DT$ s from start will differ in both the cases, causing a deviation in transient path. The magnitude of this error increases with increase in x, and the error accumulates as transient progresses. It is caused by the highly nonlinear nature of governing equations and because accuracy in tracking pressure dynamics decreases with increasing steps in time.

Also, the pressure terms in the engine state vector have varying time constants as a result of different control volume sizes. The control volume size for P_5 update (i.e., the control volume from HP turbine exit to LP turbine exit) is the smallest, and hence P_5 transient has the least time constant. Thus a uniform time scaling on all of the control volumes will again introduce error in the analysis.

After the ramp (or step) change is over, the control variables take a constant value. Because of a shorter time constant, an error in pressure dynamics alters the engine path only during the first few seconds (or until such time the control inputs are changing). It will not affect the location of the final steady-state point upon completion of the transients. But, large errors should preferably be avoided primarily to preserve the numerical stability of the analysis. It may also affect the verification and qualification of engine control system when used for hardware-in-the-loop simulation because update in control variables in closed loop is sensitive to the feedback values of N_L, N_H, T_2, P_3, and T_6.

Model Validation

The model validation is extremely important to establish the accuracy with which the model reflects the behavior of actual system. In the present case 9 s.v. model forms the base, against which the modified 6 s.v. model is validated. The validation of the 6 s.v. model in the steady state, as well as in the open- and closed-loop transient operation modes is contained in this section.

The validation of the baseline 9 s.v. model is described in Ref. 4. There is a good agreement between the model predictions and the actual engine test data at various steady-state points, right down to about 4% of maximum thrust. The model-predicted rotor speed responses at SLS during acceleration, deceleration, and a hot reslam between idle and maximum thrust also compare well with that of an experimental engine. It induces sufficient confidence in the adequacy of 9 s.v. formulation to simulate an engine's steady-state and dynamic behavior and hence its use in the present work as the baseline reference.

Steady-State Validation

A number of flight points scattered within the flight envelope of a typical fighter aircraft were chosen. At each of the flight points, a range of power settings, varying from idling (or near idling) to max power in dry as well as reheat operation mode, were chosen. The percentage deviation from baseline of important steady-state performance parameters at a few of the operating conditions in dry operation mode is presented in Tables 4–6. Similarly, Table 7 presents the performance comparison in max reheat mode at the flight points stated in Tables 4–6. BPR and SFC denote the engine bypass ratio and thrust specific fuel consumption, respectively. H is in kilometers. DT_{amb} is 20 K, except at SLS ($H = 0$, $M = 0$), where it is 0 K.

It can be seen from Tables 4–7 that the results compare fairly well. Similar error bands were observed at a large number of other operating conditions also. It confirms the adequacy of 6 s.v. model to accurately predict the engine steady-state performance.

Table 4 Steady-state performance comparison at idling

H/M	BPR	N_L	N_H	Thrust	SFC
0/0	−1.42	−0.70	−0.17	−1.65	1.63
0/0.9	−0.12	−0.11	−0.04	−0.28	0.28
3/0.6	−0.32	−0.19	−0.05	−0.59	0.59
6/0.6	−0.38	−0.34	−0.07	−1.28	1.27
9/0.9	0.01	−0.27	−0.10	0.07	−0.07
9/1.2	−0.33	−0.12	−0.02	−0.28	0.28
9/1.4	−0.07	−0.14	−0.06	0.13	−0.13
12/1.4	0.01	−0.12	−0.05	−0.67	0.66

Table 5 Steady-state performance comparison in part-power dry operation

H/M	BPR	N_L	N_H	Thrust	SFC
0/0	−0.61	−0.27	−0.04	−0.65	0.65
0/0.9	−0.66	−0.06	0.00	0.03	−0.03
3/0.6	−0.62	−0.10	−0.01	−0.15	0.15
6/0.6	−0.46	−0.12	−0.02	−0.11	0.10
9/0.9	−0.47	−0.11	−0.01	−0.11	0.11
9/1.2	−0.58	−0.09	−0.01	0.10	−0.10
9/1.4	−0.22	−0.12	−0.05	−0.12	0.12
12/1.4	−0.56	−0.08	0.00	−0.02	0.09

Table 6 Steady-state performance comparison in max-power dry operation

H/M	BPR	N_L	N_H	Thrust	SFC
0/0	−0.32	−0.04	0.00	−0.05	0.05
0/0.9	−0.25	−0.09	0.00	0.02	−0.02
3/0.6	−0.35	−0.04	0.00	−0.05	0.05
6/0.6	−0.41	−0.10	0.01	−0.03	0.03
9/0.9	−0.42	−0.10	0.01	0.01	−0.01
9/1.2	−0.17	−0.03	0.00	−0.13	0.13
9/1.4	−0.10	−0.03	0.00	−0.20	0.20
12/1.4	−0.45	0.00	0.04	0.04	−0.04

Table 7 Steady-state performance comparison in max reheat operation

$H/M/DT_{amb}$	T_7	Thrust	SFC
0/0.0/0	0.04	−0.05	0.05
0/0.9/20	0.01	0.01	−0.08
3/0.6/20	0.02	−0.06	0.06
6/0.6/20	0.03	−0.06	0.06
9/0.9/20	0.04	−0.05	0.05
9/1.2/20	0.00	0.04	−0.04
9/1.4/20	0.05	−0.02	0.02
12/1.4/20	0.03	−0.02	0.02

Transient Validation (Open Loop)

The open-loop transient at ISA, SLS, for a 4-s ramp change in control variables that corresponds to engine excursion from idling to max speed in dry operation was used to identify the possible increase in frame-time with 6 s.v. model. The next step is to establish if the increased frame times of 1.2 and 2.0 ms with time scaling of control volumes by three and five times respectively can be used for open-loop transient simulation at other flight points as well without loosing the accuracy and numerical stability. A total of four transients were chosen for this purpose, as described here:

1) $H = 3.0$ km, $M = 0.30$, ISA + 20.
2) $H = 6.0$ km, $M = 0.60$, ISA + 20.
3) $H = 6.0$ km, $M = 0.90$, ISA +20.
4) $H = 9.0$ km, $M = 1.20$, ISA + 20.

Because the ramp change in control variables is affected for 4 s to change the engine state from idling to max speed in dry operation mode, it is the first 4 or 5 s of the transients that are more critical. The deviations, if any, will be more pronounced in the initial portion of transients, subsequent to which the engine begins to settle to final steady-state point.

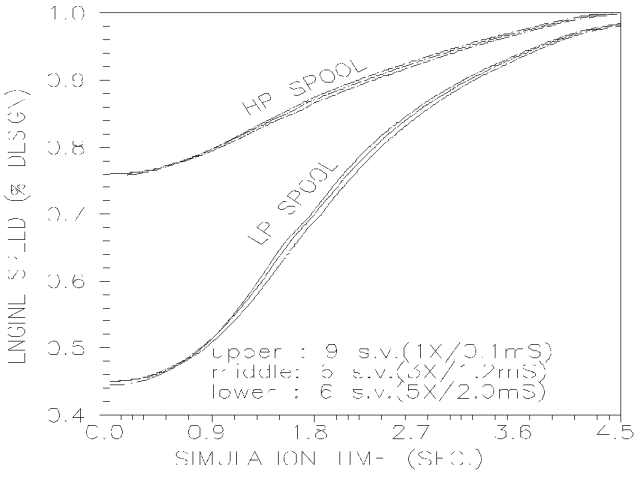

Fig. 6 Open-loop transient comparison at H = 3.0 km, M = 0.0, ISA + 20.

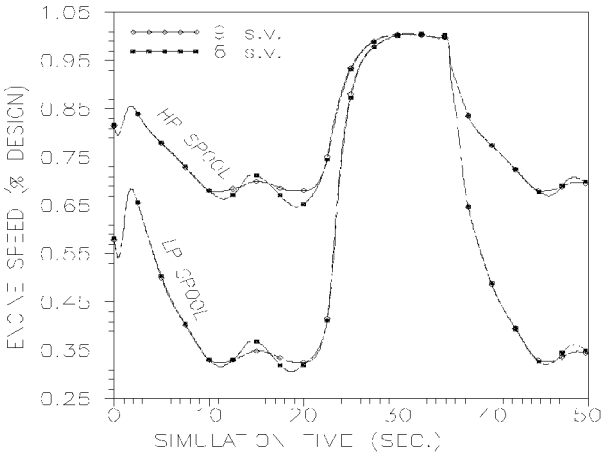

Fig. 7 Closed-loop transient comparison at ISA, SLS.

A typical comparison of the open-loop transient results between the baseline 9 s.v. and the modified 6 s.v. models is shown in Fig. 6 for the first one of the just-mentioned transient simulations. A similar comparison was observed for the remaining transient cases as well. Only the LP and HP spool speeds are shown, and the remaining parameters follow a similar trend. It can be seen that a frame time of 1.2 ms with three times the control volumes size is fairly acceptable. In case it is not suitable for real-time simulation, it can be increased to 2.0 ms, but at reduced accuracy.

Transient Validation (Closed Loop)

The modified 6 s.v. model was integrated with controller software and was run in closed loop to investigate its interactions with the control system. Because of the limitations imposed by controller software, a frame time of 0.10 ms could only be used.

Slam acceleration (idling to max speed) and deceleration (max to idling speed) were done at various flight conditions in dry operation mode. The engine was allowed to settle at idling speed during the first 20 s, after which it was slammed to max speed and allowed to settle there for next 15 s. The engine was then brought back to idling speed in the last 15 s.

The results from 6 s.v. model compared well with that from the baseline 9 s.v. model. This is evident from Fig. 7, which is for a ISA, SLS transient, and Fig. 8, which is for transient at $H = 9.0$ km, $M = 0.90$, ISA + 20. A similar good agreement was also observed at a number of other transient points as well as for reheat mode operation.

Cycle Time Vs Frame Time

The computation time as mentioned in Table 3 is the total time for a 20-s transient and illustrates the real-time capabilities of modified

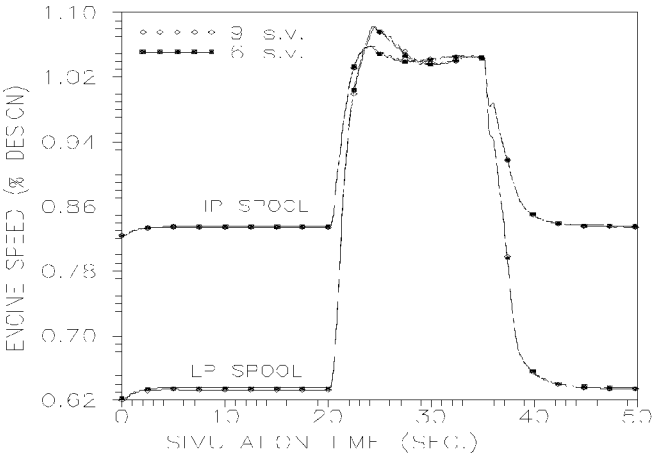

Fig. 8 Closed-loop transient comparison at H = 9.0 km, M = 0.90, ISA + 20.

6 s.v. model only on the overall basis. It is, in fact, the cycle time that is a true measure of the real-time capabilities of an engine simulation. The cycle time together with the input/output time (for interaction between the control system hardware and the real-time engine system software during hardware-in-loop simulation) must always be less than (or utmost equal to) the prescribed frame time for every engine pass if the model has to truly have the real-time capabilities. One engine pass refers to one set of calculations for generating time derivatives of state variables and updating the engine state for a prescribed disturbance in control inputs.

An initial estimate of the cycle time is given in Table 3. A 20-s transient requires 16,667 passes through the engine simulation at a frame time of 1.2 ms (20 s/1.2 ms = 16,667). Because the total computation time is 11.10 s, each pass takes 0.67 ms on an average. It is not possible to measure such a low cycle time by using the in-built clock of a Pentium III machine because the lowest time it can measure is only 50 ms. Thus, a PC-PLUS 131 timer card[5] was used for clocking the time during each engine pass. Utilizing the embedded clock frequency of 2 MHz, the minimum and maximum times this card can measure are 0.0005 and 32 ms, respectively.

The cycle time was observed to lie between 0.60–0.75 ms for a large number of speed excursions (from idling or near idling to max speed) at various flight points and for various values of frame time. It is about 0.75 ms in the early phase where transients are initiated by disturbing the control inputs and gradually reduces to 0.60 ms when engine begins to approach steady state. The present dynamic simulation is based on the noniterative control volumes approach, and a finite set of calculation are performed during each engine pass, except that number of iterations over specific heat convergence may differ between various engine passes. Thus, cycle time tends to have similar order magnitude, irrespective of the frame time and the nature of transient simulation.

Given the achievable cycle times as just stated, frame times of 0.80, 1.20, 1.60, and 2.0 ms (as listed in Table 3) are suitable for real-time digital simulation at the existing level of computation speed on a PC platform. A frame time of 1.60 or 2.0 ms shall give a better allowance for interaction between the controller hardware and real-time engine software, whereas lower frame times of 0.80 and 1.2 ms are desirable for better accuracy. A tradeoff between the available PC-based computing speed and the time required for interaction between the controller hardware and engine software will determine the actual value of usable frame time.

Conclusions

This paper describes the development of an engine thermodynamic model, the transient computational performance of which is suitable for real-time digital simulation. The engine considered is a twin-spool turbofan with reheat, involving the mixing of core and bypass streams in the main mixer. The starting point is an existing, nonlinear detailed thermodynamic simulation, termed as the baseline reference.

The baseline reference is an explicitly time-integrated engine model and uses the state variables and control volumes approach. Because of its high sensitivity on mixing-plane pressure dynamics, it requires a small frame time of 0.10 ms to produce a numerically stable and accurate transient simulation. Thus computation time taken by it is a major drawback for its real-time implementation. The high sensitivity to pressure dynamics also restricts the time scaling of control volumes to achieve any significant increase in frame time, which is one of the ways to improve the transient computational performance.

The real-time engine simulation described in this paper presents a way to overcome this limitation. It does so by retaining all of the baseline modeling features, except for that of main mixer. Instead of assuming a uniform rate of static pressure across the main mixer, it is shown that it is sufficient to assume static pressures to be uniform. It reduces the model's sensitivity to pressure dynamics and also to the time scaling of control volumes. As a result, the transient computational performance of the model improves, primarily because of its ability to use a higher frame time. It can be increased further by time scaling the control volumes.

It is now possible to use a frame time of 0.40 ms with actual control volumes and 1.2 ms with three times the time scaling of control volumes, while preserving the numerical accuracy and stability of transient analysis. The cycle time lies between 0.60–0.75 ms for a large number of transient simulations. Because the reference for cycle time is a Pentium III and it is much less compared to the frame time of 1.2 ms, the proposed formulation is suitable for real-time simulation even on a simple and cost-effective digital platform like a PC. The model results in steady-state as well as in open-loop transient operation mode compare fairly well with the baseline model. The validity of the modified model in closed-loop simulation with increased frame time is yet to be tested. It could not be done because it is the controller software that limits the frame time to 0.10 ms.

References

[1] Society of Automotive Engineers, Inc., "Real-Time Modeling Methods for Gas Turbine Engine Performance," Aerospace Information Rept., AIR 4548, Warrendale, PA, Dec. 1995.

[2] Fawke, A. J., and Saravanamuttoo, H. I. H., "Digital Computer Methods for Prediction of Gas Turbine Dynamic Response," Society of Automotive Engineers, Paper 710550, June 1971.

[3] "Design Document on Kaveri Engine Simulation," Gas Turbine Research Establishment, ITM/ES8704, Bangalore, India, Nov. 1991.

[4] Fawke, A. J., and Saravanamuttoo, H. I. H., "Digital Computer Simulation of Dynamic Response of Twin-Spool Turbofan with Mixed Exhausts," *Aeronautical Journal*, Sept. 1973, pp. 471–478.

[5] "PC-PLUS 131 Timer Card," Systems Aids, User Reference Manual, Bangalore, India, June 1996.